Nanostructures

DOI: 10.1002/ange.201107425

Tuning Complex Shapes in Platinum Nanoparticles: From Cubic Dendrites to Fivefold Stars**

Lise-Marie Lacroix, Christophe Gatel, Raul Arenal, Cécile Garcia, Sébastien Lachaize, Thomas Blon, Bénédicte Warot-Fonrose, Etienne Snoeck, Bruno Chaudret, and Guillaume Viau*

The synthesis of nanoparticles (NPs) exhibiting large surface-area-to-volume ratios has been a long-sought goal in developing various applications such as ultrasensitive sensors[1] or highly active catalysts.[2] In addition to a large specific area, crystallographic planes exposed on the surface of the NPs are key parameters for the reactivity and selectivity of NPs in catalytic processes.[3] Thus, intense research has been devoted to the shape control of noble-metal nanocrystals.[4] For example, for Pt-based nanoparticles, dendritic nanostructures,[5] branched-NPs,[6] or multipods[7] exhibit enhanced catalytic activities relative to their spherical counterparts.[8] Such shape control could be obtained by manipulating the reduction kinetics[6] through temperature,[6a,9] pH,[10] ligands,[11] or the addition of small amounts of nucleating agents.[6b] Interestingly, in this variety of shapes, only few groups reported multiply twinned Pt nanoparticles,[12] whereas decahedrons are fairly common for most of the noble metals (e.g. Au, Ag, Rh).[13] However, these twinned NPs could offer significant benefits toward catalysis because they have mainly their {111} faces exposed.[14]

Herein, we report complex platinum nanoobjects of unprecedented shapes (monodisperse cubic dendrites and fivefold stars) and the fine-tuning between two growth mechanisms. The platinum concentration is finely tuned in a fairly simple reaction of H_2PtCl_6 in oleylamine under dihydrogen pressure. Amine plays the role of solvent and stabilizer and can assist the reduction process. Previous work has shown that the room-temperature reduction of $HAuCl_4$ by neat oleylamine yielded unique Au nanowires.[15] However, in the same conditions, Pt required higher temperature to be reduced (250 °C).[9] In the present study, addition of dihydrogen, a well-known reducing agent,[16] lowered the reduction temperature and, at the same time, played an important role in the shape control of NPs. Indeed, H_2 can "clean" the NP surface by temporarily removing weak coordinating ligands, such as amines, leading to coalescence or ripening.[17] H_2 can also generate surface hydrides, which stabilize the NP and perform hydrogenation reactions.[18]

An ex situ kinetic study, followed by high-resolution transmission electron microscopy (HRTEM), has evidenced two growth mechanisms based respectively on cubic or decahedric seeds (see Scheme 1) leading to monodisperse cubic dendrites or fivefold stars.

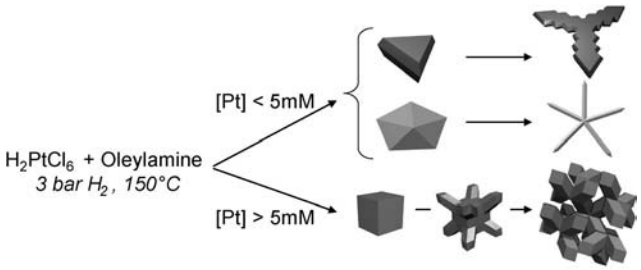

Scheme 1. General overview of the versatile synthesis of Pt^0 NPs. Shape could be controlled by the platinum concentration and the nature of the seeds formed.

Pt NPs were produced by reduction of H_2PtCl_6 in oleylamine under an H_2 atmosphere (3 bar) at 150 °C (see the Experimental Section and Scheme 1). The shape of the Pt NPs could be easily tuned by varying the experimental parameters, in particular the Pt concentration from low (2 mM) to high (10 mM) values. For example, dendritic growth was observed at high Pt concentration ([Pt] > 5 mM) (Figure 1 a,b and Figures S1 and S2 in the Supporting Information). The resulting objects were obtained quantitatively with a Pt yield over 95 %. The most striking feature, relative to previously reported dendrites,[5] was their cubic contour.

Figure 2 a shows a high-magnification transmission electron microscopy (TEM) image of a single dendrite exhibiting dense organization of branches with defined orientations. The outer faces of the cubes coincided with the {100} planes of the crystallographic structure of fcc-Pt. The selective-area electron diffraction (SAED) pattern on a single cube (Figure 2 b) shows fourfold symmetry, which is characteristic of a single-crystalline fcc crystal observed along the ⟨100⟩ zone axis. The elongation of the diffraction spots {200} and {220} indicates a slight misorientation between the branches (ca. 10°). These

[*] Dr. L.-M. Lacroix, Dr. C. Garcia, Dr. S. Lachaize, Dr. T. Blon, Prof. B. Chaudret, Prof. G. Viau
LPCNO, Université de Toulouse, INSA, UPS, CNRS
135 avenue de Rangueil, 31077 Toulouse (France)
E-mail: lmlacroi@insa-toulouse.fr
Homepage: http://lpcno.insa-toulouse.fr/
Dr. C. Gatel, Dr. B. Warot-Fonrose, Prof. E. Snoeck
CEMES, CNRS, 29 rue Jeanne Marvig, 31077 Toulouse (France)
Dr. R. Arenal
Laboratorio de microscopias avanzadas (LMA), Instituto de Nanociencia de Aragon (INA), U. Zaragoza
C/Mariano Esquillor s/n, 50018 Zaragoza (Spain)
Dr. R. Arenal
Fundacion ARAID, 50004 Zaragoza (Spain)

[**] This work was supported by the European FP7-Train2 project and the French network METSA. We thank G. Antorrena for XPS measurements.

Supporting information for this article is available on the WWW under http://dx.doi.org/10.1002/anie.201107425.

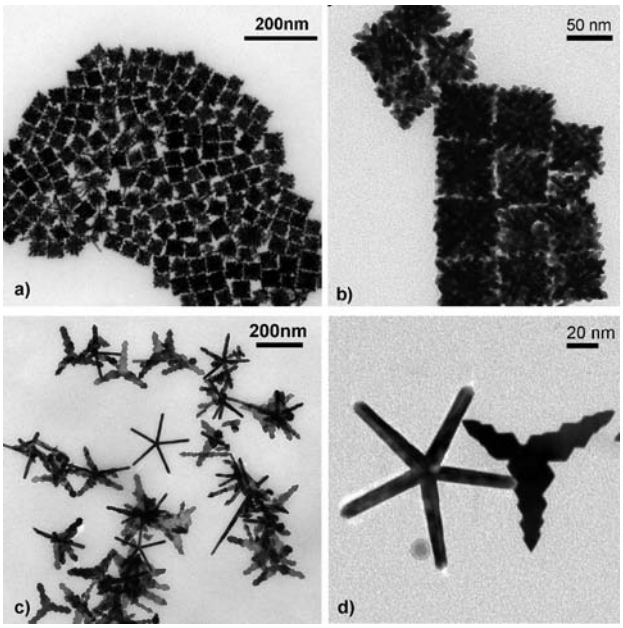

Figure 1. TEM images of Pt nanocrystals prepared at various concentrations of platinum: a,b) dendritic cubes obtained at [Pt] = 10 mM; c,d) Pt stars obtained at [Pt] = 2 mM.

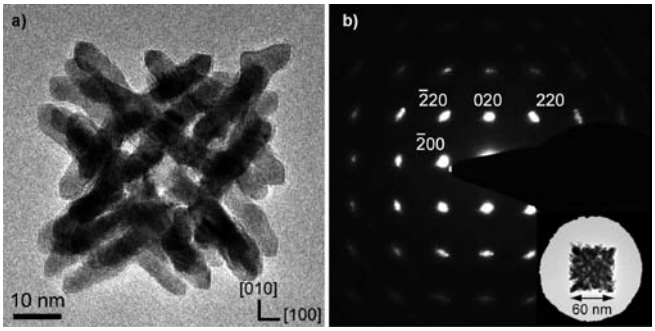

Figure 2. a) HREM image of a single Pt dendritic cube obtained after reaction for 1 h. b) SAED pattern along the [001] axis on a 60-nm-cube obtained after reaction for 2 h, as shown in the inset.

results demonstrate that cubic dendrites adopt a slightly distorted single-crystalline structure.

The growth mechanism of such peculiar dendrites was investigated by stopping the reaction at various stages (Figure 3 and Figure S3). The reaction is very fast, as shown by the octapods already observed after 1 min of reaction at 150 °C. These octapods result from a growth on the ⟨111⟩ directions on cubic seeds. The {100} facets are observed, concomitant with closing {110} facets. After 3 min of reaction, the selected growth on {100} facets leads to the appearance of bifurcations, and new branches start to grow along three different ⟨111⟩ growth directions. Such selected growth is repeated until the platinum precursor is completely consumed. Although the diameter of the branches was rather constant at approximately 5.5 nm, the mean size of the cubic dendrites could be tuned from 30 to 100 nm by varying the reaction time between 10 min and 2 h (Figure S4). The dendrites finally obtained exhibit a high proportion of {100}

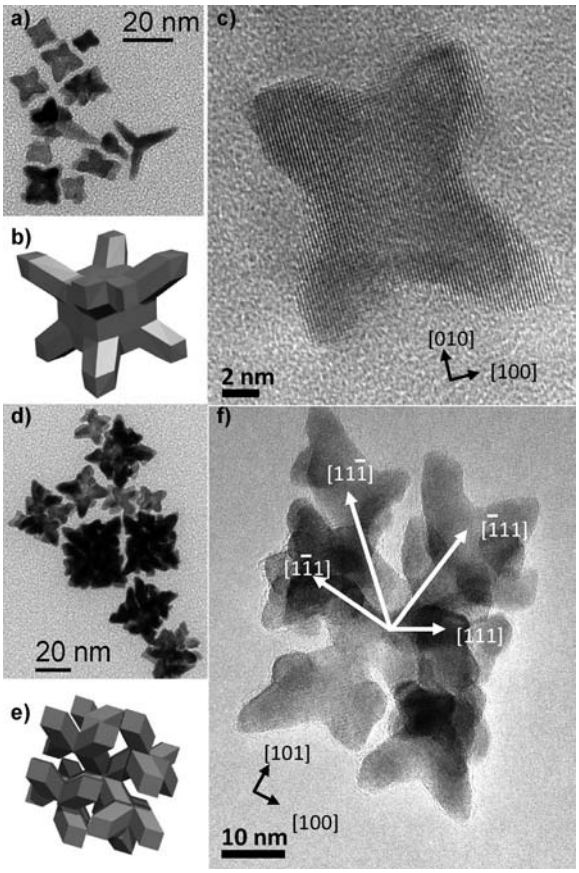

Figure 3. Nanoparticles obtained after reaction for a–c) 1 min and d–f) 3 min. a,d) TEM micrograph and the corresponding c,f) HREM micrographs. The {100} facets are highlighted along the ⟨111⟩ growth directions. b,e) Schematic view of the objects at this growth stage.

and {110} facets, as in the earlier growth stage (Figure S5). Such dendritic structures, which have no precedent, were stable at 150 °C for days; the complex branches architecture did not collapse into denser crystals.

Star-shaped NPs were obtained at low Pt concentration ([Pt] = 2 mM; Figure 1 c,d and Figure S6). Samples were composed of nanocrystals exhibiting a well-defined morphology with around 20 % fivefold stars, 70 % threefold stars (planar tripods), and 10 % multipods or undefined shapes. This ratio could vary: the proportion of multipods increased with the [Pt] concentration. Threefold stars were obtained previously by using a different approach (reduction of $Pt(acac)_2$ by a diol at 160 °C).[7a] However, the present fivefold Pt stars are unique. Their arm length could be tuned from 30 nm to 120 nm by varying the reaction time between 6 and 48 h (Figure S7).

Figure 4 shows a high magnification image of a single fivefold star and the corresponding SAED pattern along the ⟨110⟩ zone axis. The complex pattern displays fivefold symmetry of the fcc structure spots, which is similar to the SAED pattern obtained on Au decahedra.[19] The HRTEM image of the core clearly shows the noncrystallographic fivefold axis and the five resulting twinning boundaries. Periodic lattice fringes could be clearly resolved for three families of planes.

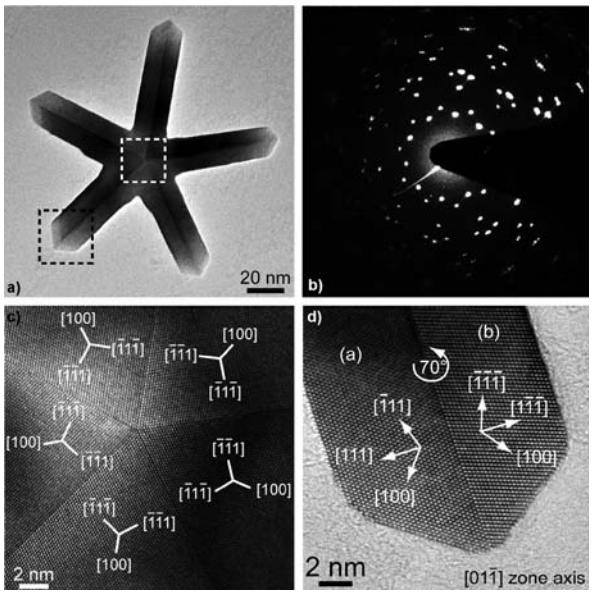

Figure 4. a) TEM micrograph of a single Pt fivefold star and b) its corresponding ED pattern. HRTEM images of c) the core and d) a branch tip as shown in (a) by white and black boxes, respectively.

Lattice spacings of 2.26 Å and 1.96 Å correspond to the {111} and {100} planes of fcc-Pt, respectively. The rotation of these planes along the fivefold axis is evidenced in Figure 4c: single-crystalline tetrahedra were observed between two successive twin boundaries.

Figure 4d shows a HRTEM image of the branch tip. The branches are highly crystalline, exposing mainly {111} facets (Figures S8–10). These branches grow symmetrically along the twinning plane from each corner of the central decahedra, as revealed by TEM images taken after different growth stages (Figure 5). Such growth on decahedra corners was

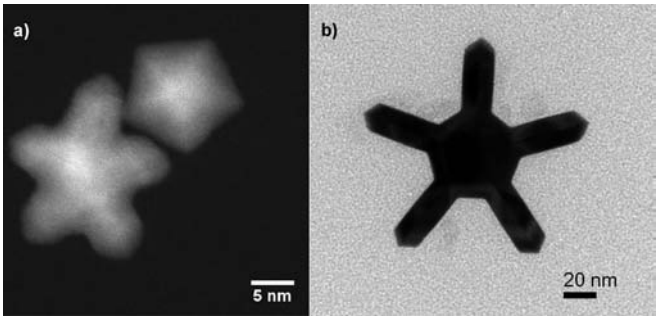

Figure 5. High-angle annular dark field and TEM images of Pt NPs obtained for [Pt] = 2 mM after reaction for a) 2 h and b) 4 h.

recently reported by Zhang et al. on Rh starfishlike NPs, but the crystallinity of the branches was not clearly evidenced.[13c] If Pt decahedra are fairly rare objects, highly crystalline fivefold Pt stars represent a unique result to the best of our knowledge.

X-ray photoelectron spectroscopy (XPS) and energy-dispersive X-ray spectroscopy (EDS) analyses were performed on cubic dendrites and stars. As expected, the Pt NPs resulting from the different syntheses consisted of pure Pt^0 (Figures S11–12). The surface of the particles was stabilized mostly by amine groups, although chloride anions and ammonium groups could be detected as traces.

It is noteworthy that reaction times were considerably longer at low [Pt] concentration compared with the few minutes required for high [Pt] concentration synthesis. At 2 mM, the yellow color, which is characteristic of the Pt precursor, vanished after at least 24 h of reaction. The shape control in this versatile synthesis then looked strongly correlated with the reaction rates. Three experimental parameters can be adjusted to increase the reaction rate: [Pt] concentration, temperature (T), and dihydrogen pressure (p_{H_2}). Increasing the temperature and pressure yield cubic dendrites after only 1 hour (Figure S13), even at low [Pt] concentration (2 mM). Thus, we could induce a dendritic growth by increasing the reaction rate. An illustration of this difference of kinetic between cubic dendrites and stars is given by the variation of dihydrogen pressure profile with time (Figure S14). Fast consumption of dihydrogen was observed for dendritic growth, while no abrupt drop was detected in the case of star-shaped growth. These two hydrogenation profiles combine multiple reactions (reduction of platinum, corresponding to ca. 0.3 bar of H_2, and hydrogenation catalyzed by Pt NPs or molecular species) in various experimental conditions. Thus, the catalytic activities of dendrites vs. stars cannot be directly compared. However, we can conclude that very catalytically active species were quickly formed at high temperature and pressure, whereas this was not the case under conditions of lower temperature and pressure.

The shape control reported herein for Pt^0 NPs (planar tripods, fivefold stars, and cubic dendrites) was achieved by varying the reaction conditions in a relatively narrow range of concentration or temperature. The nature of the seeds—cubic (exposing noncompact faces) or triangular and decahedric (exposing {111} faces)—is determinant in the final morphology reached (Scheme 1).

At fast reaction rates, cubic seeds, exhibiting fcc structure, are quickly formed as shown by ex situ HREM study and the evolution of H_2 pressure as a function of time. The very fast consumption of H_2 is due to fast reduction of Pt precursor and to the hydrogenation of oleylamine by reactive seeds. Noncompact faces ({100} and {110}) are known to be active towards the reduction of internal olefins for Pd.[20] These cubic seeds, although very reactive, are relatively limited in number. The stability of the H_2PtCl_6 precursor is indeed a determinant factor in this dendritic growth. The reduction of $Pt(acac)_2$ under similar conditions yielded multiple seeds and thus multiarmed NPs (Figure S15). Few seeds and fast reduction is characteristic of an autocatalytic process, previously reported for Pt.[3] Such autocatalytic processes combines a surface reaction between the precursor and preferential faces, leading here to a growth direction along ⟨111⟩ directions. The outer cubic shape of these nearly single-crystalline cubic dendrites, so peculiar, results from the strong crystallographic driving force combined with the tendency of dihydrogen to repair surfaces. The large cubic dendrites obtained at the end of the reaction expose noncompact faces,

which are not energetically favored. Such structures represent kinetic products and result from a growth limited by the diffusion of adatoms at the surface. Such diffusion-limited process is also known to be responsible for the size monodispersity of the final objects.[21]

When the reaction rates were decreased, by lowing either the platinum concentration or the reaction temperature, the reduction of the platinum precursor occurred over a longer period of time and yielded seeds exhibiting compact {111} faces. The profile of dihydrogen consumption is drastically modified compared to dendritic growth, as a result of the formation of a very limited number of seeds and of their nature. Indeed, under these conditions, stable twinned decahedra or triangular seeds could grow, resulting from the minimization of surface energy. These objects expose only {111} compact crystallographic planes. The successive growth of decahedra seeds into fivefold stars could be explained through multiple nucleation events. Decahedra are composed of five tetrahedra. However, these tetrahedra cannot fill the entire space and leave an empty angle of 7.3°, unless they adopt a highly strained structure, as reported for Au decahedra.[19] Since strain increases with the particle size, above a critical size, corresponding to the highest strain in Pt decahedron, the structure relaxes. In our case, this relaxation corresponds to the nucleation and growth of the arms at each corner of the decahedra core (Figure 5). Further crystallographic studies will be performed on these fivefold stars to determine the structural strain contained in the vicinity of the core and of the arms to confirm our growth model hypothesis. Such a multistep process has already been proposed by Maksimuk et al.[12a] for the growth of planar tripods. According to their model, branches grow at the corner of triangular twinned seeds, which act as preferential nucleation sites for a second growth process. In our reaction, fivefold stars and planar tripods coexist, giving strength to our growth hypothesis.

In summary, we have demonstrated that quasi-single-crystalline Pt nanoparticles with peculiar morphologies—cubic dendrites, planar tripods, and fivefold stars—can be obtained selectively and in high yield from a very simple procedure by tuning the reduction kinetics of a platinum salt under a dihydrogen atmosphere in the presence of an amine. The control of experimental parameters such as Pt concentration, reaction temperature, and dihydrogen pressure, leads to fine-tuning of the kinetics of the reaction and of the nature of seeds formed during the nucleation step. Although the reason for such an abrupt transition between cubic or twinned seeds is still unknown, numerical simulations of the energy of the seeds could give some important insights.

A slow reaction leads to twinned seeds, which evolve into planar tripods (threefold stars) and fivefold stars. Such multiply twinned NPs are unique for Pt and could open new perspectives for fundamental research on strained materials. In addition to this fundamental interest, catalytic activities could benefit from the presence of almost exclusively crystallographic surface orientation {111} for selectivity purposes.

A fast reaction leads to cubic seeds and thus to a dendritic growth. The peculiarity of these objects is their outer cubic shape and an unprecedented size control of their envelope. Such dendritic cubes display a high surface-to-volume ratio, while their cubic shape enables their self-assembly on surfaces, which should be of high interest in catalysis. Structural characterization of the exposed surfaces, the reactivity, and the catalytic activity of these novel species will be evaluated to attest the potential of these unique cubic dendrites.

Experimental Section

Typical synthesis of dendritic NPs : H_2PtCl_6 (Alfa Aesar, 51 mg, 0.1 mmole) and oleylamine (Aldrich, 10 mL) were mixed in a vial and placed for 15 min in an ultrasonic bath to dissolve the Pt precursor. The 10 mM solution was transferred in a Fisher–Porter bottle and pressurized up to 3 bar with H_2. The bottle was then allowed to react at 150 °C in a preheated oil bath for 1 h. At the end of the reaction, a black precipitate was obtained while the supernatant is transparent. Typical yellow Pt precursor traces were no longer observed. The bottle was then cooled to room temperature, resulting in solidification of the supernatant. Hexanes (40 mL, Aldrich) was added to solubilize the NPs. The suspension, after the addition of 40 mL of absolute ethanol (VWR), was then centrifuged (4000 rpm, 6 min) to separate the NPs. The process is repeated three times to remove the excess of surfactants. The final product (ca. 25 mg) was kept in powder form or diluted in 5 mL toluene (Carlo Erba) for further use.

Multiply twinned NPs were synthesized by a similar procedure except that the Pt concentration was decreased below 5 mM. The reaction time was extended to 48 h, because the reaction rate is drastically reduced.

Characterization: Samples for TEM analysis were prepared by depositing few drops of diluted solution on an amorphous carbon-coated cupper grid. Low-resolution images were obtained with a JEOL-1400 microscope, operating at 120 kV. HRTEM images were obtained with a Tecnai F20 (200 kV) instrument equipped with a spherical aberration corrector. X-ray photoelectron spectra were recorded using a Kratos Analytical Limited Axis ultralimited system fitted with a microfocused monochromatic $Al_{K\alpha}$ X-ray source (1486.6 eV, 12 kV × 120 W). The pass energy was set at 160 eV and 20 eV for the survey and the regions spectra, respectively.

Received: October 21, 2011
Revised: March 7, 2012
Published online: March 30, 2012

Keywords: crystal growth · nanostructures · platinum · solid-state structures

[1] N. J. Wittenberg, C. L. Haynes, *WIREs Nanomed. Nanobiotech.* **2009**, *1*, 237–254.
[2] a) R. J. White, R. Luque, V. L. Budarin, J. H. Clark, D. J. Macqarrie, *Chem. Soc. Rev.* **2009**, *38*, 481–494; b) E. Antolini, J. Perez, *J. Mater. Sci.* **2011**, *46*, 4435–4457.
[3] J. Chen, B. Lim, E. P. Lee, Y. Xia, *Nano Today* **2009**, *4*, 81–95.
[4] a) A. R. Tao, S. Habas, P. Yang, *Small* **2008**, *4*, 310–325; b) T. K. Sau, A. L. Rogach, *Adv. Mater.* **2010**, *22*, 1781–1804.
[5] a) Y. Song, Y. Yang, C. J. Madforth, E. Pereira, A. K. Singh, H. Xu, Y. Jiang, C. J. Brinker, F. Van Swol, J. A. Schelnutt, *J. Am. Chem. Soc.* **2004**, *126*, 635–645; b) X. Zhong, Y. Feng, I. Lieberwirth, W. Knoll, *Chem. Mater.* **2006**, *18*, 2468–2471.
[6] a) J. Ren, R. D. Tilley, *Small* **2007**, *3*, 1508–1512; b) J. Chen, T. Herricks, Y. Xia, *Angew. Chem.* **2005**, *117*, 2645–2648; *Angew. Chem. Int. Ed.* **2005**, *44*, 2589–2592.

[7] a) M. A. Mahmoud, C. E. Tabor, M. A. El-Sayed, Y. Ding, Z. L. Wang, *J. Am. Chem. Soc.* **2008**, *130*, 4590 – 4591; b) S. Sun, G. Zhang, D. Geng, Y. Chen, R. Li, M. Cai, X. Sun, *Angew. Chem.* **2011**, *123*, 442 – 446; *Angew. Chem. Int. Ed.* **2011**, *50*, 422 – 426.
[8] a) Z. Peng, H. Yang, *Nano Today* **2009**, *4*, 143 – 164; b) B. Lim, Y. Xia, *Angew. Chem.* **2011**, *123*, 78 – 87; *Angew. Chem. Int. Ed.* **2011**, *50*, 76 – 85.
[9] H.-T. Zhang, J. Ding, G.-M. Chow, *Langmuir* **2008**, *24*, 375 – 378.
[10] H. Lee, S. E. Habas, S. Kweskin, D. Butcher, G. A. Somorjai, P. Yang, *Angew. Chem.* **2006**, *118*, 7988 – 7992; *Angew. Chem. Int. Ed.* **2006**, *45*, 7824 – 7828.
[11] M. R. Axet, K. Philippot, B. Chaudret, M. Cabié, S. Giorgio, C. R. Henry, *Small* **2011**, *7*, 235 – 241.
[12] a) S. Maksimuk, X. Teng, H. Yang, *J. Phys. Chem. C* **2007**, *111*, 14312 – 14319; b) N. V. Long, M. Ohtaki, M. Uchida, R. Jalem, H. Hirata, N. D. Chien, M. Nogami, *J. Colloid Interface Sci.* **2011**, *359*, 339 – 350.
[13] a) D. Seo, C. I. Yoo, I. S. Chung, S. M. Park, S. Ryu, H. Song, *J. Phys. Chem. C* **2008**, *112*, 2469 – 2475; b) W. Zhang, Y. Liu, R. Cao, Z. Li, Y. Zhang, Y. Tang, K. Fan, *J. Am. Chem. Soc.* **2008**, *130*, 15581 – 15588; c) H. Zhang, X. Xia, W. Li, J. Zeng, Y. Dai, D. Yang, Y. Xia, *Angew. Chem.* **2010**, *122*, 5424 – 5428; *Angew. Chem. Int. Ed.* **2010**, *49*, 5296 – 5300.
[14] a) A. Guerrero-Martínez, S. Barbosa, I. Pastoriza-Santos, L. M. Liz-Marzan, *Curr. Opin. Colloid Interface Sci.* **2011**, *16*, 118 – 127; b) H. Hofmeister, *Z. Kristallogr.* **2009**, *224*, 528 – 538.
[15] a) Z. Huo, C.-K. Tsung, W. Huang, X. Zhang, P. Yang, *Nano Lett.* **2008**, *8*, 2041 – 2044; b) X. Lu, M. S. Yavuz, H.-Y. Tuan, B. A. Korgel, Y. Xia, *J. Am. Chem. Soc.* **2008**, *130*, 8900 – 8901.
[16] a) F. Dumestre, B. Chaudret, C. Amiens, M. Respaud, P. Fejes, P. Renaud, P. Zurcher, *Angew. Chem.* **2003**, *115*, 5371 – 5374; *Angew. Chem. Int. Ed.* **2003**, *42*, 5213 – 5216; b) L.-M. Lacroix, S. Lachaize, A. Falqui, M. Respaud, B. Chaudret, *J. Am. Chem. Soc.* **2009**, *131*, 549 – 557; c) C. Desvaux, C. Amiens, P. Fejes, P. Renaud, M. Respaud, P. Lecante, E. Snoeck, B. Chaudret, *Nat. Mater.* **2005**, *4*, 750 – 753.
[17] E. Ramirez, L. Eradès, K. Philippot, P. Lecante, B. Chaudret, *Adv. Funct. Mater.* **2007**, *17*, 2219 – 2228.
[18] a) T. Pery, K. Pelzer, G. Buntkowsky, K. Philippot, H.-H. Limbach, B. Chaudret, *ChemPhysChem* **2005**, *6*, 605 – 607; b) J. García-Antón, M. R. Axet, S. Jansat, K. Philippot, B. Chaudret, T. Pery, G. Buntkowsky, H.-H. Limbach, *Angew. Chem.* **2008**, *120*, 2104 – 2108; *Angew. Chem. Int. Ed.* **2008**, *47*, 2074 – 2078.
[19] C. L. Johnson, E. Snoeck, M. Ezcurdia, B. Rodriguez-Gonazalez, I. Pastoriza-Santos, L. M. Liz-Marzan, M. J. Hÿtch, *Nat. Mater.* **2008**, *7*, 120 – 124.
[20] a) L. Piccolo, A. Valcarel, M. Bausach, C. Thomazeau, D. Uzio, G. Berhault, *Phys. Chem. Chem. Phys.* **2008**, *10*, 5504 – 5506; b) D. Uzio, G. Berhault, *Catal. Rev. Sci. Eng.* **2010**, *52*, 106 – 131.
[21] J. Park, J. Joo, S. G. Kwon, Y. Jang, T. Hyeon, *Angew. Chem.* **2007**, *119*, 4714 – 4745; *Angew. Chem. Int. Ed.* **2007**, *46*, 4630 – 4660.

